



# Fermi National Accelerator Laboratory

DART-HEP-97/05 – October 1997

Fermilab-Conf-97/324-A – October 1997

## Phase Transitions: An Overview with a View <sup>1</sup>

*Marcelo Gleiser<sup>2</sup>*

Department of Physics and Astronomy  
Dartmouth College, Hanover, NH 03755, USA <sup>3</sup>

and

Nasa/Fermilab Astrophysics Center  
Fermi National Accelerator Laboratory  
Batavia, IL 60510

and

LAFEX-Centro Brasileiro de Pesquisas Físicas  
Urca, Rio de Janeiro, RJ, Brasil

### Abstract

The dynamics of phase transitions plays a crucial rôle in the so-called interface between high energy particle physics and cosmology. Many of the interesting results generated during the last fifteen years or so rely on simplified assumptions concerning the complex mechanisms typical of nonequilibrium field theories. After reviewing well-known results concerning the dynamics of first and second order phase transitions, I argue that much is yet to be understood, in particular in situations where homogeneous nucleation theory does not apply. I present a method to deal with departures from homogeneous nucleation, and compare its efficacy with numerical simulations. Finally, I discuss the interesting problem of matching numerical simulations of stochastic field theories with continuum models.

---

<sup>1</sup>Invited plenary talk given at "Fundamental Physics at the Birth of the Universe II", Rome, 19-24 May 1997.

<sup>2</sup>NSF Presidential Faculty Fellow

<sup>3</sup>Permanent address



## **Disclaimer**

*This report was prepared as an account of work sponsored by an agency of the United States Government. Neither the United States Government nor any agency thereof, nor any of their employees, makes any warranty, express or implied, or assumes any legal liability or responsibility for the accuracy, completeness, or usefulness of any information, apparatus, product, or process disclosed, or represents that its use would not infringe privately owned rights. Reference herein to any specific commercial product, process, or service by trade name, trademark, manufacturer, or otherwise, does not necessarily constitute or imply its endorsement, recommendation, or favoring by the United States Government or any agency thereof. The views and opinions of authors expressed herein do not necessarily state or reflect those of the United States Government or any agency thereof.*

## **Distribution**

*Approved for public release: further dissemination unlimited.*

# 1 Part I: Homogeneous Nucleation

The fact that the gauge symmetries describing particle interactions can be restored at high enough temperatures has led, during the past 15 years or so, to an active research program on the possible implications that this symmetry restoration might have had to the physics of the very early Universe. One of the most interesting and popular possibilities is that during its expansion the Universe underwent a series of phase transitions, as some higher symmetry group was successively broken into products of smaller groups, up to the present standard model described by the product  $SU(3)_C \otimes SU(2)_L \otimes U(1)_Y$ . Most models of inflation and the formation of topological (and nontopological) defects are well-known consequences of taking the existence of cosmological phase transitions seriously [1].

One, but certainly not the only, motivation of the works addressed in this talk comes from the possibility that the baryon asymmetry of the Universe could have been dynamically generated during a first order electroweak phase transition [2]. As is by now clear, a realistic calculation of the net baryon number produced during the transition is a formidable challenge. We probably must invoke physics beyond the standard model (an exciting prospect for most people), push perturbation theory to its limits (and beyond, due to the nonperturbative nature of magnetic plasma masses that regulate the perturbative expansion in the symmetric phase), and we must deal with nonequilibrium aspects of the phase transition. Here I will focus on the latter problem, as it seems to me to be the least discussed of the pillars on which most baryon number calculations are built upon. To be more specific, it is possible to separate the nonequilibrium aspects of the phase transition into two main subdivisions. If the transition proceeds by bubble nucleation, we can study the propagation of bubbles in the hot plasma and the transport properties of particles through the bubble wall. A considerable amount of work has been devoted to this issue, and the reader can consult the works of Ref. [3] for details. These works assume that homogeneous nucleation theory is adequate to investigate the evolution of the phase transition, at least for the range of parameters of interest in the particular model being used to generate the baryon asymmetry. This brings us to the second important aspect of the nonequilibrium dynamics of first order phase transitions, namely the validity of homogeneous nucleation theory to describe the approach to equilibrium. This is the issue addressed in this talk.

Nucleation theory is a well-studied, but far from exhausted, subject. Since the pioneering work of Becker and Döring on the nucleation of droplets in supercooled vapor [4], the study of first order phase transitions has been of interest to investigators in several fields, from meteorology and materials science to quantum field theory and cosmology. Phenomenological field theories were developed by Cahn and Hilliard and by Langer [5, 6] in the context of coarse-grained time-dependent Ginzburg-Landau models, in which an expression for the decay rate per unit volume was obtained by assuming a steady-state probability current flowing through the saddle-point of the free-energy functional [6, 7]. The application of metastable decay to quantum field theory was initiated by Voloshin, Kobzarev, and Okun [8], and soon after put onto firmer theoretical ground by Coleman and Callan [9]. The generalization of these results for finite temperature field theory was first studied by Linde [10], and has been the focus of much recent attention [11].

The crucial ingredient in the evaluation of the decay rate is the computation of the imaginary part of the free energy. As shown by Langer [6], the decay rate  $\mathcal{R}$  is proportional to the imaginary part of the free energy  $\mathcal{F}$ ,

$$\mathcal{R} = \frac{|E_-|}{\pi T} \text{Im}\mathcal{F} , \quad (1)$$

where  $E_-$  is the negative eigenvalue related to metastability, which depends on nonequilibrium aspects of the dynamics, such as the growth rate of the critical bubble. Since  $\mathcal{F} = -T \ln Z$ , where  $Z$  is the partition function, the computation for the rate boils down to the evaluation of the partition function for the system comprised of critical bubbles of the lower energy phase inside the metastable phase.

If we imagine the space of all possible field configurations for a given model, there will be different paths to go from the metastable to the ground state. We can think of the two states as being separated by a hill of a given “height”. The energy barrier for the decay is then related to the height of this hill. At the top of the hill, only one direction leads down to the ground state, the unstable direction. Fluctuations about this direction will grow, with rate given by the negative eigenvalue which appears in the above formula. All other directions are positively curved, and fluctuations about them give rise to positive eigenvalues which do not contribute to the decay rate. The path which will cost less energy is the one which will dominate the partition function, the so-called critical bubble or bounce. It is simply

the field configuration that interpolates between the two stable points in the *energy landscape*, the metastable and ground state. The energy barrier for the decay is the energy of this particular field configuration.

For a dilute gas of bubbles only, the partition function for several bubbles is given by [12, 6],

$$\begin{aligned} Z &\simeq Z(\varphi_f) + Z(\varphi_f) \left[ \frac{Z(\varphi_b)}{Z(\varphi_f)} \right] + Z(\varphi_f) \frac{1}{2!} \left[ \frac{Z(\varphi_b)}{Z(\varphi_f)} \right]^2 + \dots \\ &\simeq Z(\varphi_f) \exp \left[ \frac{Z(\varphi_b)}{Z(\varphi_f)} \right], \end{aligned} \quad (2)$$

where  $\varphi_f$  is the metastable vacuum field configuration and  $\varphi_b$  is the bubble configuration, the bounce solution to the  $O(3)$ -symmetric Euclidean equation of motion. We must evaluate the partition functions above. This is done by the saddle-point method, expanding the scalar field  $\phi(\mathbf{x}, \tau)$ , such that  $\phi(\mathbf{x}, \tau) \rightarrow \varphi_f + \zeta(\mathbf{x}, \tau)$  for  $Z(\varphi_f)$ , and  $\phi(\mathbf{x}, \tau) \rightarrow \varphi_b(\mathbf{x}) + \eta(\mathbf{x}, \tau)$  for  $Z(\varphi_b)$ , where  $\zeta(\mathbf{x}, \tau)$  and  $\eta(\mathbf{x}, \tau)$  are small fluctuations about equilibrium.

It is crucial to note that the saddle-point, or Gaussian, method only gives good results if indeed the fluctuations about equilibrium are sufficiently small that nonlinear terms in the fields can be neglected. Even though the method sums over all amplitude fluctuations, it does so by assuming that the functional integral is well approximated by truncating the expansion of the action to second order. The efficiency of the method relies on the fact that higher amplitudes will be suppressed fast enough that their contribution to the partition function will be negligible. One can visualize this by comparing a sharp parabolic curve with a flatter one with minimum at  $x_0$ , and investigating when  $\int dx e^{-f(x)}$  will be well approximated by writing  $f(x) \simeq f(x_0) + \frac{1}{2}(x - x_0)^2 f''(x_0)$ . For a sharp curve, larger amplitude fluctuations will be strongly suppressed and thus give a negligible contribution to the integral over all amplitudes. Clearly, this will not be the case for flatter curves.

Skipping details [11], using the saddle-point method one obtains for the ratio of partition functions,  $\frac{Z(\varphi_b)}{Z(\varphi_f)}$ ,

$$\frac{Z(\varphi_b)}{Z(\varphi_f)} \stackrel{\text{saddle-point}}{\simeq} \left[ \frac{\det(-\square_E + V''(\varphi_b))_\beta}{\det(-\square_E + V''(\varphi_f))_\beta} \right]^{-\frac{1}{2}} e^{-\Delta S}, \quad (3)$$

where  $[\det(M)_\beta]^{-\frac{1}{2}} \equiv \int D\eta \exp \left\{ - \int_0^\beta d\tau \int d^3x \frac{1}{2} \eta [M] \eta \right\}$  and  $\Delta S = S_E(\varphi_b) - S_E(\varphi_f)$  is the difference between the Euclidean actions for the field configurations  $\varphi_b$  and  $\varphi_f$ . [Note that  $S_E(\varphi)$ , and hence  $\Delta S$ , does not include any temperature corrections. It would if one had summed over other fields coupled to  $\varphi$ .] Thus, the free energy of the system is,

$$\mathcal{F} = -T \left[ \frac{\det(-\square_E + V''(\varphi_b))_\beta}{\det(-\square_E + V''(\varphi_f))_\beta} \right]^{-\frac{1}{2}} e^{-\Delta S}. \quad (4)$$

Let me stress again the assumptions that go into computing the free energy. First, that the partition function is given by Eq. 2 within the dilute gas approximation, and second, that the partition function is evaluated approximately by assuming *small* fluctuations about the homogeneous metastable state  $\varphi_f$ . It is clear that for situations in which there are large amplitude fluctuations about the metastable equilibrium state the above formula must break down. Thus the breakdown of the expression for the rate is intimately connected with the question of how well-localized the system is about the metastable state as the temperature drops below the critical temperature  $T_c$ . Homogeneous nucleation, as its name already states, is only accurate when the metastable state is sufficiently homogeneous. In the presence of inhomogeneities, there is no reason to expect that the decay rate formula will apply. The question then is to quantify *when* does it break down and how can we incorporate nonperturbative corrections to the decay rate in a consistent way.

## 2 Part II: Nonperturbative corrections to decay rates

In order to investigate the importance of large-amplitude fluctuations in the description of first order phase transitions, I have developed numerical simulations in two [13] and, with J. Borrill, three [14] spatial dimensions, which measured the fraction of the volume of the system in the initial phase as a function of the barrier height. Since these have been documented elsewhere, here I quickly describe the main idea and results.

Imagine a scalar field with a degenerate double-well potential. The field is coupled to a thermal bath at temperature  $T$  through a Langevin-like equa-

tion which assumes that the bath is Markovian, *i.e.*, the noise is white and additive. The system is artificially divided into two regions, left and right of the maximum of the potential, call it the negative and positive regions, respectively. The system is prepared initially in one of the regions, say, the negative region with  $\phi(\mathbf{x}, t = 0) = -1$ . The coupling to the bath will then drive fluctuations of the field around this minimum and we measure the fraction of the total volume in each of the two regions as a function of the parameters controlling the height of the potential barrier, usually the temperature and/or a coupling constant.

We observed that while for large enough potential barriers the system remained well-localized around its initial state, a sharp change of behavior occurred for a critical value of the specific control parameter being varied. In the case examined in Ref. [14], the control parameter was the quartic coupling of the scalar field,  $\lambda$ . We showed that for  $\lambda > \lambda_c$  the system became completely mixed, in that the volume was equally shared by the positive and negative regions. In other words, for  $\lambda > \lambda_c$ , the effective potential describing the system is not a degenerate double-well, but a parabolic curve centered at  $\langle \phi \rangle = 0$ ; Thermal fluctuations have “restored” the symmetry of the system.

The challenge was thus to model the large amplitude fluctuations which were responsible for this phase mixing. In what follows I review the so-called subcritical bubbles method which can model *quantitatively* the dynamics of large, nonperturbative, thermal fluctuations in scalar field theories.

## 2.1 Modeling nonperturbative fluctuations: Symmetry Restoration

As was stressed before, the computation of decay rates based on homogeneous nucleation theory assumes a smooth metastable background over which critical bubbles of the lower free energy phase will appear, grow and coalesce, as the phase transition evolves. However, as the results from the numerical simulations indicate, the assumption of smoothness is not always valid. To the skeptical reader, I point out that several condensed matter experiments indicate that homogeneous nucleation fails to describe the transition when the nucleation barrier ( $\Delta S/T$ ) becomes too small. Furthermore, the agreement between theory and experiment has a long and problematic history [15]. Homogeneous nucleation has to be used with care, in a case by case basis.

The basic idea is that in a hot system, not only small but also large amplitude fluctuations away from equilibrium will, in principle, be present. Small amplitude fluctuations are perturbatively incorporated in the evaluation of the finite temperature effective potential, following well-known procedures. Large amplitude fluctuations probing the nonlinearities of the theory are not. Whenever they are important, the perturbative effective potential becomes unreliable. In an ideal world, we should be able to sum over all amplitude fluctuations to obtain the exact partition function of the model, and thus compute the thermodynamic quantities of interest. However, we can only do this perturbatively, and will always miss information coming from the fluctuations not included in its evaluation. If large amplitude fluctuations are strongly suppressed, they will not contribute to the partition function, and we are in good shape. But what if they are important, as argued above? We can try to approach this question avoiding complicated issues related to the evaluation of path integrals beyond the Gaussian approximation by obtaining a kinetic equation which describes the fraction of volume populated by these large amplitude fluctuations. In order to keep the treatment simple, and thus easy to apply, several assumptions are made along the way, which I believe are quite sensible. In any case, the strength of the method is demonstrated when the results are compared with the numerical experiments described before.

Large amplitude fluctuations away from equilibrium are modelled by Gaussian-profile spherically-symmetric field configurations of a given size and amplitude. They can be thought of as being coreless bubbles. Keeping with the notation of the numerical experiment, fluctuations away from the 0-phase, and into the 0-phase are written respectively as,

$$\phi_c(r) = \phi_c e^{-r^2/R^2}, \quad \phi_0(r) = \phi_c (1 - e^{-r^2/R^2}), \quad (5)$$

where  $R$  is the radial size of the configuration, and  $\phi_c$  is the value of the amplitude at the bubble's core, away from the 0-phase. In previous treatments (cf. Refs. [16] and [17]), it was assumed that  $\phi_c = \phi_+$ , that is, that the configuration interpolated between the two minima of the effective potential, and that  $R = \xi(T)$ , where  $\xi(T) = m(T)^{-1}$  is the mean-field correlation length. But in general, one should sum over all radii and amplitudes above given values which depend on the particular model under study. This will become clear as we go along.

Define  $dn(R, \phi, t)$  as the number density of bubbles of radius between  $R$  and  $R + dR$  at time  $t$ , with amplitudes  $\phi \geq \phi_c$  between  $\phi$  and  $\phi + d\phi$ . By choosing to sum over bubbles of amplitudes  $\phi_c$  and larger, we are effectively describing the system as a “two-phase” system. For example, in the numerical simulation above it was assumed that the negative-phase was for amplitudes  $\phi \leq \phi_{\max}$ , and the positive-phase was for amplitudes  $\phi > \phi_{\max}$ . Clearly, for a continuous system this division is artificial. However, since the models we are interested in have two local minima of the free energy, this division becomes better justified. Fluctuations with small enough amplitude about the minima are already summed over in the computation of the effective potential. It is the large amplitude ones which are of relevance here. To simplify the notation, from now on I will denote by “+ phase” all fluctuations with amplitudes  $\phi > \phi_c$  and larger. The choice of  $\phi_c$  is model-dependent, as will be clear when we apply this formalism to specific examples.

The fact that the bubbles shrink will be incorporated in the time dependence for the radius  $R^4$ . Here, I will only describe a somewhat simplified approach to the dynamics. More details are provided in the work by Gleiser, Heckler, and Kolb [19]. The results, however, are essentially identical.

The net rate at which bubbles of a given radius and amplitude are created and destroyed is given by the kinetic equation,

$$\begin{aligned} \frac{\partial n(R, t)}{\partial t} = & -\frac{\partial n(R, t)}{\partial R} \left( \frac{dR}{dt} \right) + \left( \frac{V_-}{V_T} \right) \Gamma_{- \rightarrow +}(R) \\ & - \left( \frac{V_+}{V_T} \right) \Gamma_{+ \rightarrow -}(R) \end{aligned} \quad (6)$$

Here,  $\Gamma_{- \rightarrow +}(R)$  ( $\Gamma_{+ \rightarrow -}(R)$ ) is the rate per unit volume for the thermal nucleation of a bubble of radius  $R$  of positive-phase within the negative-phase (negative-phase within the positive-phase).  $V_{-(+)}$  is the volume available for nucleating bubbles of the  $+(-)$  phase. Thus we can write, for the total volume of the system,  $V_T = V_- + V_+$ , expressing the fact that the system has been “divided” into two available phases, related to the local minima of the free energy density. It is convenient to define the fraction of volume in the + phase,  $\gamma$ , as

---

<sup>4</sup>Of course, the amplitude  $\phi$  will also be time-dependent. However, its time-dependence is coupled to that of the radius, as recent studies have shown [18]. In order to describe the effect of shrinking on the population of bubbles it is sufficient to include only the time dependence of the radius.

$$\frac{V_+}{V_T} \equiv 1 - \gamma \quad . \quad (7)$$

In order to compute  $\gamma$  we must sum over *all* bubbles of different sizes, shapes, and amplitudes within the  $+$  phase, *i.e.*, starting with  $\phi_{\min} \geq \phi_c$ . Clearly, we cannot compute  $\gamma$  exactly. But it turns out that a very good approximation is obtained by assuming that the bubbles are spherically symmetric, and with radii above a given minimum radius,  $R_{\min}$ . The reason we claim that the approximation is good comes from comparing the results of this analytical approach with numerical simulations. The approximation starts to break down as the background becomes more and more mixed, and the morphology of the “bubbles” becomes increasingly more important, as well as other terms in the kinetic equation which were ignored. For example, there should be a term which accounts for bubble coalescence, which increases the value of  $\gamma$ . This term becomes important when the density of bubbles is high enough for the probability of two or more of them coalescing to be non-negligible. As we will see, by this point the mixing is already so pronounced that we are justified in neglecting this additional complication to the kinetic equation. As a bonus, we will be able to solve it analytically. The expression for  $\gamma$  is,

$$\gamma \simeq \int_{\phi_{\min}}^{\infty} \int_{R_{\min}}^{\infty} \left( \frac{4\pi R^3}{3} \right) \frac{\partial^2 n}{\partial \phi \partial R} d\phi dR \quad . \quad (8)$$

The attentive reader must have by now noticed that we have a coupled system of equations;  $\gamma$ , which appears in the rate equation for the number density  $n$ , depends on  $n$  itself. And, to make things even worse, they both depend on time. Approximations are in order, if we want to proceed any further along an analytical approach. The first thing to do is to look for the equilibrium solutions, obtained by setting  $\partial n / \partial t = 0$  in the kinetic equation. In equilibrium,  $\gamma$  will also be constant<sup>5</sup>. If wished, after finding the equilibrium solutions one can find the time-dependent solutions, as was done in Ref. [17]. Here, we are only interested in the final equilibrium distribution of subcritical bubbles, as opposed to the approach to equilibrium.

---

<sup>5</sup>This doesn't mean that thermal activity in or between the two phases is frozen; equilibrium is a statement of the average distribution of thermodynamical quantities. Locally, bubbles will be created and destroyed, but always in such a way that the average value of  $n$  and  $\gamma$  are constant.

The first approximation is to take the shrinking velocity of the bubbles to be constant,  $dR/dt = -v$ . This is in general not the case (*cf.* Ref. [18]), but it does encompass the fact that subcritical bubbles shrink into oblivion. The strength of the thermodynamic approach is that details of how the bubbles disappear are unimportant, only the time-scale playing a rôle. The second approximation is to assume that the rates for creation and destruction of subcritical fluctuations are Boltzmann suppressed, so that we can write them as  $\Gamma = AT^4 e^{-F_{\text{sc}}/T}$ , where  $A$  is an arbitrary constant of order unity, and  $F_{\text{sc}}(R, \phi_c)$  is the cost in free energy to produce a configuration of given radius  $R$  and core amplitude  $\phi_c$ . For the Gaussian *ansatz* we are using,  $F_{\text{sc}}$  assumes the general form,  $F_{\text{sc}} = \alpha R + \beta R^3$ , where  $\alpha = b\phi_c^2$  ( $b$  is a combination of  $\pi$ 's and other numerical factors) and  $\beta$  depends on the particular potential used. In practice, the cubic term can usually be neglected, as the free energy of small ( $R \sim \xi$ ) subcritical bubbles is dominated by the gradient (linear) term. We chose to look at the system at the critical temperature  $T_c$ . For this temperature, the creation and destruction rates,  $\Gamma_{\rightarrow+}$  and  $\Gamma_{+\rightarrow-}$  are identical. Also, for  $T_c$ , the approximation of neglecting the cubic term is very good (in fact it is better and better the larger the bubble is) even for large bubbles, since for degenerate vacua there is no gain (or loss) of volume energy for large bubbles. Finally, we use that  $V_+/V_T = \gamma$  in the  $\Gamma_{+\rightarrow-}$  term. A more sophisticated approach is presented in Ref. [19].

We can then write the equilibrium rate equation as,

$$\frac{\partial n}{\partial R} = -cf(R) \quad , \quad (9)$$

where,

$$c \equiv (1 - 2\gamma)AT^4/v, \quad f(R) \equiv e^{-F_{\text{sc}}/T} \quad . \quad (10)$$

Integrating from  $R_{\text{min}}$  and imposing that  $n(R \rightarrow \infty) = 0$ , the solution is easily found to be,

$$n(R) = \frac{c}{\alpha(\phi_c)/T} e^{-\alpha(\phi_c)R/T} \quad . \quad (11)$$

Not surprisingly, the equilibrium number density of bubbles is Boltzmann suppressed. But we now must go back to  $\gamma$ , which is buried in the definition of  $c$ . We can solve for  $\gamma$  perturbatively, by plugging the solution for  $n$  back into Eq. 8. After a couple of fairly nasty integrals, we obtain,

$$\gamma = \frac{g(\alpha(\phi_{\min}), R_{\min})}{1 + 2g(\alpha(\phi_{\min}), R_{\min})} , \quad (12)$$

where,

$$g(\alpha(\phi_{\min}), R_{\min}) = \frac{4\pi}{3} \left( \frac{AT^4}{v} \right) \left( \frac{T}{\alpha} \right)^3 \frac{e^{-\alpha R_{\min}/T}}{\alpha/T} \left[ 6 + \left( \frac{\alpha R_{\min}}{T} \right)^3 + 3 \frac{\alpha R_{\min}}{T} \left( 2 + \frac{\alpha R_{\min}}{T} \right) \right] . \quad (13)$$

We can now apply this formalism to any model we wish. The first obvious application is to compare  $\gamma$  obtained from the numerical experiment with the value obtained from the kinetic approach. From the definition of the equilibrium fractional population difference,  $\Delta F_{\text{EQ}}(\theta_c) \equiv f_0^{\text{eq}} - f_+^{\text{eq}}$ ,

$$\Delta F_{\text{EQ}}(\theta_c) = 1 - 2\gamma . \quad (14)$$

Thus, it is straightforward to extract the value of  $\gamma$  from the numerical simulations as a function of  $\lambda$ . Also, as we neglected the volume contribution to the free energy of subcritical bubbles, we have,

$$F_{sc} = \alpha(\phi_c) R_{\min} = \frac{3\sqrt{2}}{8} \pi^{3/2} X_-^2(\theta_c) R_{\min} , \quad (15)$$

where, as you recall,  $X_-$  is the position of the maximum of the mean-field potential used in the simulations. So, we must sum over all amplitudes with  $X \geq X_-$ , and all radii with  $R \geq 1$  (in dimensionless units), as we took the lattice spacing to be  $\ell = 1$ . That is, we sum over all possible sizes, down to the minimum cut-off size of the lattice used in the simulations. In practice, we simply substitute  $\phi_c = X_-$  and  $R_{\min} = 1$  in the expression for  $\gamma$ . In Fig. 1, we compare the numerical results for  $\gamma$  (dots) with the results from the analytical integration of the kinetic equation. We plots are for different values of the parameter  $A/v$ . Up to the critical value for  $\lambda \simeq 0.025$ , the agreement is very convincing. As we increase  $\lambda$  into the mixed phase region of the diagram, the kinetic approach underestimates the amount of volume in the  $+$ -phase. This is not surprising, since for these values of  $\lambda$  the density of subcritical bubbles is high enough that terms not included in the equation become important, as I mentioned before. However, the lack of agreement for higher values of  $\lambda$  is irrelevant, if we are interested in having a measure of the smoothness of the background; clearly, the rise in  $\gamma$  is sharp enough

that homogeneous nucleation should not be trusted for  $\lambda > 0.024$  or so, as the fraction of volume occupied by the  $+$ -phase is already around 30% of the total volume. Subcritical bubbles give a simple and quantitatively accurate picture of the degree of inhomogeneity of the background, offering a guideline as to when homogeneous nucleation theory can be applied with confidence, or, alternatively, when the effective potential needs higher order corrections.

## 2.2 Modeling nonperturbative fluctuations: “Inhomogeneous” nucleation

Now we apply the subcritical bubbles method to the decay of metastable states in the case that the homogeneous nucleation formalism (Part I) does not apply. Details of this work can be found in Ref. [21].

As mentioned before, if there is significant phase mixing in the background metastable state, its free-energy density is no longer  $V(\phi = 0)$ , where I assume the potential has a metastable state at  $\phi = 0$ . One must also account for the free-energy density of the nonperturbative, large-amplitude fluctuations. Since there is no formal way of deriving this contribution outside improved perturbative schemes, we propose to estimate the corrections to the background free-energy density by following another route. We start by writing the free energy density of the metastable state as  $V(\phi = 0) + \mathcal{F}_{\text{sc}}$ , where  $\mathcal{F}_{\text{sc}}$  is the nonperturbative contribution to the free-energy density due to the large amplitude fluctuations, which we assume can be modelled by subcritical bubbles. We will calculate  $\mathcal{F}_{\text{sc}}$  further below.

We thus define the effective free-energy difference between the two minima,  $\Delta V_{\text{cg}}$ , which includes corrections due to phase mixing, as

$$\Delta V_{\text{cg}} = \Delta V_0 + \mathcal{F}_{\text{sc}} \quad (16)$$

which is the sum of the free-energy difference calculated in the standard way, and the “extra” free-energy density due to the presence of subcritical bubbles. Henceforth, the subscript ‘cg’ will stand for “coarse-grained”.

Since for degenerate potentials (temperature-dependent or not) no critical bubbles should be nucleated, taking into account subcritical bubbles must lead to a change in the coarse-grained free-energy density (or potential) describing the transition. Thus, it should be possible to translate the “extra” free energy available in the system due to the presence of subcritical bubbles

in the background into a corrected potential for the scalar order parameter. We will write this corrected potential as  $V_{\text{cg}}(\phi)$ .

The standard coarse-grained free energy is calculated by integrating out the short-wavelength modes (usually up to the correlation length) from the partition function of the system, and is approximated by the familiar form [20]

$$F_{\text{cg}}(\phi) = \int d^3r \left( \frac{1}{2}(\nabla\phi)^2 + V_{\text{cg}}(\phi) \right). \quad (17)$$

How do we estimate  $V_{\text{cg}}$ ? One way is to simply constrain it to be consistent with the thin wall limit. That is, as  $V_{\text{cg}}(\phi)$  approaches degeneracy (*i.e.*  $\Delta V_{\text{cg}}(\phi) \rightarrow 0$ ), it must obey the thin wall limit of eq. (16). Note that with a simple rescaling, a general polynomial potential (to fourth order) can be written in terms of one free parameter. Thus, the thin wall constraint can be used to express the corrected value of this parameter in terms of  $\mathcal{F}_{\text{sc}}$  in appropriate units. The free energy of the critical bubble is then obtained by finding the bounce solution to the equation of motion  $\nabla^2\phi - dV_{\text{cg}}(\phi)/d\phi = 0$  by the usual shooting method, and substituting this solution into eq. (17).

In order to determine  $V_{\text{cg}}$ , we must first calculate the free-energy density  $\mathcal{F}_{\text{sc}}$  of the subcritical bubbles. From the formalism presented in the previous subsection,

$$\mathcal{F}_{\text{sc}} \approx \int_{\phi_{\text{min}}}^{\infty} \int_{R_{\text{min}}}^{R_{\text{max}}} F_{\text{sb}} \frac{\partial^2 n(R, t)}{\partial R \partial \phi_A} dR d\phi_A, \quad (18)$$

where  $\phi_{\text{min}}$  defines the lowest amplitude within the +phase, typically (but not necessarily) taken to be the maximum of the double-well potential.  $R_{\text{min}}$  is the smallest radius for the subcritical bubbles, compatible with the coarse-graining scale. For example, it can be a lattice cut-off in numerical simulations, or the mean-field correlation length in continuum models. As for  $R_{\text{max}}$ , it is natural to choose it to be the critical bubble radius.

As an application of the above method, we investigated nucleation rates in the context of a 2-d model for which accurate numerical results are available [22]. This allowed us to compare the results obtained by incorporating subcritical bubbles into the calculation of the decay barrier with the results from the numerical simulations. The potential used was written in terms of one dimensionless parameter  $\lambda \equiv m^2 h / g^2$ ,

$$V(\phi) = \frac{1}{2}\phi^2 - \frac{1}{6}\phi^3 + \frac{\lambda}{24}\phi^4. \quad (19)$$

This double-well potential is degenerate when  $\lambda = 1/3$ , and the second minimum is lower than the first when  $\lambda < 1/3$ .

As argued before, we find the new coarse-grained potential  $V_{\text{cg}}$  (or, equivalently,  $\lambda_{\text{cg}}$ ) by constraining it to agree with the thin wall limit. Simple algebra from eqs. (16) and (19) yields, to first order in the deviation from degeneracy,

$$\lambda_{\text{cg}} = \lambda - \frac{\tilde{\mathcal{F}}_{\text{sc}}}{54} \quad (20)$$

where  $\tilde{\mathcal{F}}_{\text{sc}} = \frac{g^2}{m^6} \mathcal{F}_{\text{sc}}$  is the dimensionless free-energy density in subcritical bubbles. The new potential  $V_{\text{cg}}$  is then used to find the bounce solution and the free energy of the critical bubble.

In Fig. 2 we show that the calculation of the nucleation barrier including the effects of subcritical bubbles is consistent with data from lattice simulations, whereas the standard calculation overestimates the barrier by a large margin. In fact, the inclusion of subcritical bubbles provides a reasonable explanation for the anomalously high nucleation rates observed in the simulations close to degeneracy.

### 3 Part III: Matching numerical simulations to continuum field theories

As a final topic to be discuss in this lecture, I would like to change gears and briefly turn to the issue of how to match numerical simulations of field theories with their continuum counterparts. In particular, I am interested in situations where a degree of stochasticity is present in the simulations, as for example happens when we model the coupling of fields to a thermal or quantum bath via a Langevin-like equation, or even in the form of noisy initial conditions.

Although field theories are continuous and usually formulated in an infinite volume, lattice simulations are discrete and finite, imposing both a maximum (“size of the box”  $L$ ) and a minimum (lattice spacing  $\delta x$ ) wavelength that can be probed by the simulation. When the system is coupled to an external thermal (or quantum) bath, fluctuations will be constrained within the allowed window of wavelengths, leading to discrepancies between

the continuum formulation of the theory and its lattice simulations; the results will be dependent on the choice of lattice spacing.

Parisi suggested that if proper counterterms were used, this dependence on lattice spacing could be attenuated [23]. Recently, Borrill and Gleiser (BG) have examined this question within the context of 2-d critical phenomena [24]. They have computed the counterterms needed to render the simulations independent of lattice spacing and have obtained a match between the simulations and the continuum field theory, valid within the one-loop approximation used in their approach. Here, I want to focus mostly on the application of these techniques to 1-d field theories, in particular to the problem of thermal nucleation of kink-antikink pairs. [This is based on work of Ref. [25].]

Even though 1-d field theories are free of ultra-violet divergences, the ultra-violet cutoff imposed by the lattice spacing will generate a *finite* contribution to the effective potential which must be taken into account if we are to obtain a proper match between the theory and its numerical simulation on a discrete lattice. If neglected, this contribution may compromise the measurement of physical quantities such as the density of kink-antikink pairs or the effective kink mass.

For classical, 1-dimensional finite-temperature field theories, the one-loop corrected effective potential is given by the momentum integral [23]

$$V_{1L}(\phi) = V_0(\phi) + \frac{T}{2} \int_0^\infty \frac{dk}{2\pi} \ln \left[ 1 + \frac{V_0''(\phi)}{k^2} \right] = V_0(\phi) + \frac{T}{4} \sqrt{V_0''(\phi)}. \quad (21)$$

As mentioned before, the lattice spacing  $\delta x$  and the lattice size  $L$  introduce long and short momentum cutoffs  $\Lambda = \pi/\delta x$  and  $k_{\min} = 2\pi/L$ , respectively. Lattice simulations are characterized by one dimensionless parameter, the number of degrees of freedom  $N = L/\delta x$ . For sufficiently large  $L$  one can neglect the effect of  $k_{\min}$  and integrate from 0 to  $\Lambda$ . For  $V_0'' \ll \Lambda^2$  (satisfied for sufficiently large  $\Lambda$ ), the result can be expanded into

$$V_{1L}(\phi, \Lambda) = V_0 + \frac{T}{4} \sqrt{V_0''} - \frac{T}{4\pi} \frac{V_0''}{\Lambda} + \Lambda T \mathcal{O} \left( \frac{V_0''^2}{\Lambda^4} \right). \quad (22)$$

As is to be expected for a 1-dimensional system, the limit  $\Lambda \rightarrow \infty$  exists and is well-behaved; there is no need for renormalization of ultra-violet divergences. However, the effective one-loop potential is lattice-spacing dependent

through the explicit appearance of  $\Lambda$ , and so are the corresponding numerical simulations. In order to remove this dependence on  $\delta x$ , we follow the renormalization procedure given by BG [24]; it is irrelevant if the  $\Lambda$ -dependent terms are ultra-violet finite ( $d = 1$ ) or infinite ( $d \geq 2$ ). In the lattice formulation of the theory, we add a (finite) counterterm to the tree-level potential  $V_0$  to remove the lattice-spacing dependence of the results,

$$V_{\text{ct}}(\phi) = \frac{T}{4\pi} \frac{V_0''(\phi)}{\Lambda}. \quad (23)$$

There is an additional,  $\Lambda$ -independent, counterterm which was set to zero by an appropriate choice of renormalization scale. The lattice simulation then uses the corrected potential

$$V_{\text{latt}}(\phi) = V_0(\phi) + \frac{T\delta x}{4\pi^2} V_0''(\phi). \quad (24)$$

Note that the above treatment yields two novel results. First, that the use of  $V_{\text{latt}}$  instead of  $V_0$  gets rid of the dependence of simulations on lattice spacing. [Of course, as  $\delta x \rightarrow 0$ ,  $V_{\text{latt}} \rightarrow V_0$ . However, this limit is often not computationally efficient.] Second, that the effective interactions that are simulated must be compared to the one-loop corrected potential  $V_{1\text{L}}(\phi)$  of Eq. (21); once the lattice formulation is made independent of lattice spacing by the addition of the proper counterterm(s), it simulates, within its domain of validity, the thermally corrected one-loop effective potential.

Applying this method to the formation of kink-antikink pairs, we get a corrected potential,

$$V_{\text{latt}}(\phi) = V_0(\phi) + \frac{3}{4\pi^2} \lambda T \delta x \phi^2; \quad (25)$$

simulations using  $V_{\text{latt}}$  will, in principle, match the continuum theory

$$V_{1\text{L}}(\phi) = V_0(\phi) + \frac{T\sqrt{\lambda}}{4} \sqrt{3\phi^2 - \phi_0^2}, \quad (26)$$

which has (shifted) minima at  $\pm\phi_{\text{min}}(T)$ , with  $\phi_{\text{min}}(T) < \phi_0$ .

As a first test of our procedure, we investigate the mean field value  $\bar{\phi}(t) = (1/L) \int \phi(x, t) dx$  *before* the nucleation of a kink-antikink pair, *i.e.*, while the field is still well localized in the bottom of the well. In Fig. 3 we show

the ensemble average of  $\bar{\phi}$  (after 100 experiments) for different values of  $\delta x$ , ranging from 1 down to 0.1, at  $T = 0.1$ . The simulations leading to the left graphs use the “bare” potential  $V_0$ , whereas the right graphs are produced employing  $V_{\text{att}}$  (Eq. 25).

Perhaps the most difficult task when counting the number of kink-antikink pairs that emerge during a simulation is the identification of what precisely is a kink-antikink pair at different temperatures. Typically, we can identify three “types” of fluctuations: i) small amplitude, perturbative fluctuations about one of the two minima of the potential; ii) full-blown kink-antikink pairs interpolating between the two minima of the potential; iii) nonperturbative fluctuations which have large amplitude but not quite large enough to satisfy the boundary conditions required for a kink-antikink pair. These latter fluctuations are usually dealt with by a smearing of the field over a certain length scale. Basically, one chooses a given smearing length  $\Delta L$  which will be large enough to “iron out” these “undesirable” fluctuations but not too large that actual kink-antikink pairs are also ironed-out. The choice of  $\Delta L$  is, in a sense, more an art than a science, given our ignorance of how to handle these nonperturbative fluctuations.

The smearing was implemented as a low pass filter with filtering cut-off  $\Delta L$ ; the field is Fourier transformed, filtered at a given wavelength, and Fourier transformed back. We counted pairs by identifying the zeros of the filtered field. Choosing the filter cutoff length to be too large may actually undercount the number of pairs. Choosing it too low may include nonperturbative fluctuations as pairs. We chose  $\Delta L = 3$  in the present work, as this is the smallest “size” for a kink-antikink pair. In contrast, in the works by Alexander et al. a different method was adopted, that looked for zero-crossings for eight lattice units (they used  $\delta x = 0.5$ ) to the left and right of a zero crossing [26]. We have checked that our simulations reproduce the results of Alexander et al. if we: i) use the bare potential in the lattice simulations and ii) use a large filter cutoff length  $\Delta L$ . Specifically, the number of pairs found with the bare potential for  $T = 0.2$ ,  $\delta x = 0.5$  are:  $n_p = 36$ , 30, and 27, for  $\Delta L = 3$ , 5, and 7 respectively. Alexander et al. found (for our lattice length)  $n_p = 25$ . Comparing results for different  $\Delta L$ , it is clear that the differences between our results and those of Alexander et al. come from using a different potential in the simulations, *viz.* a dressed vs. a bare potential. For small  $\delta x$  these differences disappear.

Fig. 4 compares measurements of the kink-antikink pair density (half the

number of zeros of the smeared field), ensemble-averaged over 100 experiments, for different lattice spacings. Again it is clear from the graphs on the left that using the tree-level potential  $V_0$  in the simulations causes the results to be dependent on  $\delta x$ , whereas the addition of the finite counterterm removes this problem quite efficiently.

Another step is to establish what is the continuum theory being simulated. Due to space limitations, I refer the reader to the work of Ref. [25] for more details.

I would like to thank Franco Occhionero for another great meeting and for his kind hospitality.

This work was written while the author was visiting the Brazilian Center for Physics Research (CBPF) and the Nasa/Fermilab Astrophysics Center. I thank both centers for their hospitality. The author was supported in part by the National Science Foundation through a Presidential Faculty Fellows Award no. PHY-9453431 and by the National Aeronautics and Space Administration through grant no. NAGW-4270. At Fermilab, I acknowledge support from DOE and by the NASA grant NAG5-2788.

## References

- [1] E. Kolb and M. Turner, *The Early Universe* (Addison-Wesley, New York, 1990).
- [2] A. G. Cohen, D. B. Kaplan, and A. E. Nelson, *Annu. Rev. Nucl. Part. Sci.* **43**, 27 (1993); A. Dolgov, *Phys. Rep.* **222**, 311 (1992).
- [3] B. Liu, L. McLerran, and N. Turok, *Phys. Rev.* **D46**, 2668 (1992); A. G. Cohen, D. B. Kaplan, and A. E. Nelson, *Phys. Lett.* **B336**, 41 (1994); M. B. Gavela, P. Hernández, J. Orloff, and O. Pène, *Mod. Phys. Lett.* **A9**, 795 (1994); P. Huet and E. Sather, *Phys. Rev.* **D51**, 379 (1994).
- [4] R. Becker and W. Döring, *Ann. Phys.* **24**, 719 (1935).
- [5] J. W. Cahn and J. E. Hilliard, *J. Chem. Phys.* **31**, 688 (1959).
- [6] J. S. Langer, *Ann. Phys. (NY)* **41**, 108 (1967); *ibid.* **54**, 258 (1969).

- [7] J. D. Gunton, M. San Miguel and P. S. Sahni, in *Phase Transitions and Critical Phenomena*, **Vol. 8**, Ed. C. Domb and J. L. Lebowitz (Academic Press, London, 1983).
- [8] M. B. Voloshin, I. Yu. Kobzarev, and L. B. Okun', *Yad. Fiz.* **20**, 1229 (1974) [*Sov. J. Nucl. Phys.* **20**, 644 (1975)].
- [9] S. Coleman, *Phys. Rev.* **D15**, 2929 (1977); C. Callan and S. Coleman, *Phys. Rev.* **D16**, 1762 (1977).
- [10] A. D. Linde, *Phys. Lett.* **70B**, 306 (1977); *Nucl. Phys.* **B216**, 421 (1983); [Erratum: **B223**, 544 (1983)].
- [11] M. Gleiser, G. Marques, and R. Ramos, *Phys. Rev.* **D48**, 1571 (1993); D. E. Brahm and C. Lee, *Phys. Rev.* **D49**, 4094 (1994); D. Boyanovsky, D. E. Brahm, R. Holman, and D.-S. Lee, *Nucl. Phys.* **B441**, 609 (1995).
- [12] P. Arnold and L. McLerran, *Phys. Rev.* **D36**, 581 (1987); *ibid.* **D37**, 1020 (1988).
- [13] M. Gleiser, *Phys. Rev. Lett.* **73**, 3495 (1994).
- [14] J. Borrill and M. Gleiser, *Phys. Rev.* **D51**, 4111 (1995).
- [15] E.D. Siebert and C.M. Knobler, *Phys. Rev. Lett.*, **52**, 1133 (1984); J.S. Langer and A.J. Schwartz, *Phys. Rev.* **A21**, 948 (1980); A. Leggett in *Helium Three*, ed. by W.P. Halperin and L.P. Pitaevskii, (North-Holland, New York, 1990); for an (outdated) review of the situation in the early eighties see Ref. [7].
- [16] M. Gleiser, E. W. Kolb, and R. Watkins, *Nucl. Phys.* **B364**, 411 (1991); G. Gelmini and M. Gleiser, *Nucl. Phys.* **B419**, 129 (1994); M. Gleiser and E. W. Kolb, *Phys. Rev. Lett.* **69**, 1304 (1992); N. Tetradis, *Z. Phys.* **C57**, 331 (1993).
- [17] G. Gelmini and M. Gleiser in Ref. [16].
- [18] M. Gleiser, *Phys. Rev.* **D49**, 2978 (1994); E.J. Copeland, M. Gleiser, and H.-R. Müller, *Phys. Rev.* **D52**, 1920 (1995).
- [19] M. Gleiser, A. Heckler, and E.W. Kolb, *Phys. Lett.* **B405** (1997) 121.

- [20] J.S. Langer, *Physica* **73**, 61 (1974).
- [21] A. Heckler and M. Gleiser, *Phys. Rev. Lett.* **76**, 180–183 (1996).
- [22] M. Alford and M. Gleiser, *Phys. Rev.* **D48**, 2838–2844 (1993).
- [23] G. Parisi, *Statistical Field Theory* (Addison-Wesley, New York, 1988).
- [24] J. Borrill and M. Gleiser, *Nucl. Phys.* **B483**, 416–428 (1997).
- [25] M. Gleiser and H.-R. Müller, Dartmouth preprint no. DART-HEP-97/04, submitted to *Physical Review Letters*, hep-lat/9704005.
- [26] F. J. Alexander and S. Habib, *Phys. Rev. Lett.* **71**, 955 (1993); F. J. Alexander, S. Habib, and A. Kovner, *Phys. Rev. E* **48**, 4282 (1993); S. Habib, cond-mat/9411058.

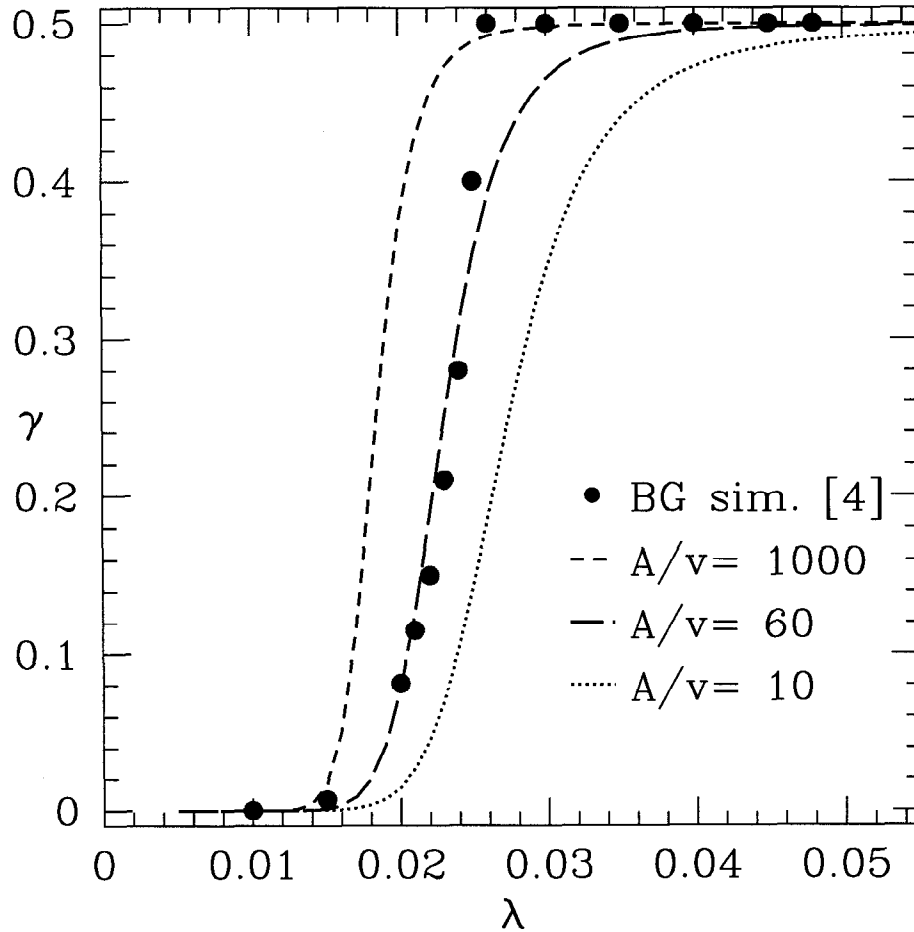


Figure 1: The fraction of the volume in the + phase. The dots are from numerical simulations of Ref. [14], while the lines are the solutions of the Boltzmann eq. for different values of the parameter  $A/|v|$ .

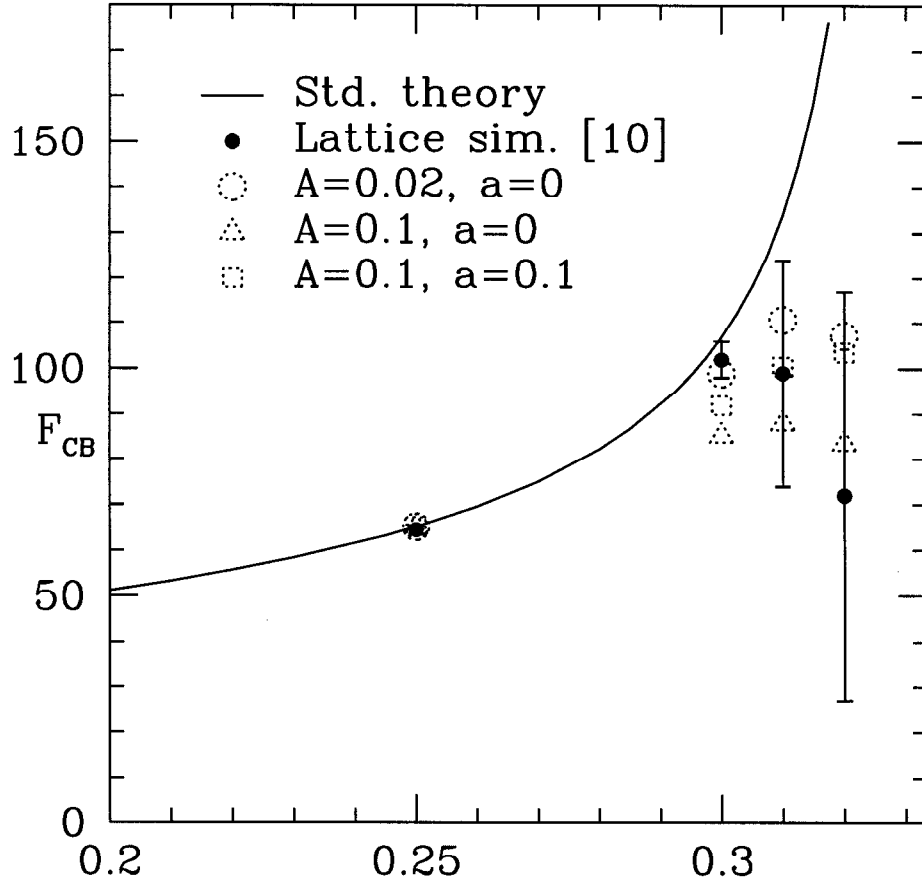


Figure 2: Comparison between numerical data and theoretical predictions for the decay barrier with and without the inclusion of subcritical bubbles. The parameter  $a$  is related to an extra term in the Boltzmann eq. which can be safely neglected.

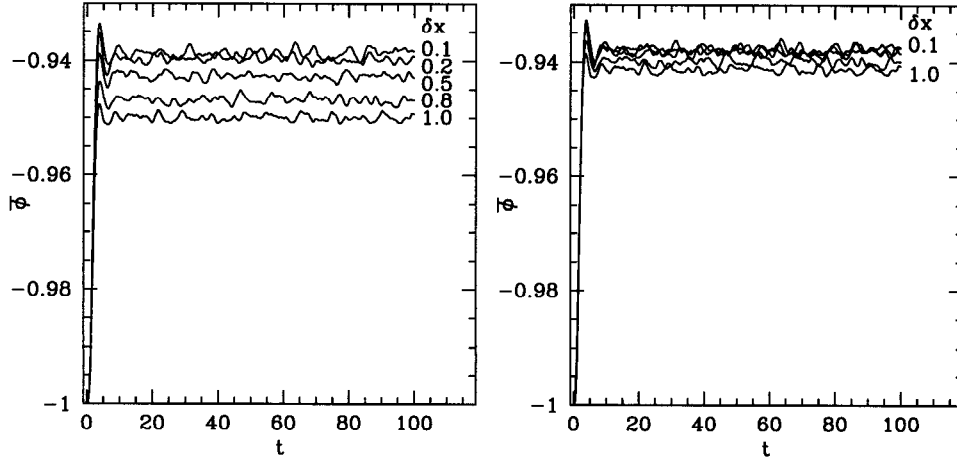


Figure 3: Average field value  $\bar{\phi}(t)$  for  $T = 0.1$  using the tree-level potential, left, and the corrected potential, right. The filter cutoff is  $\Delta L = 3$ .

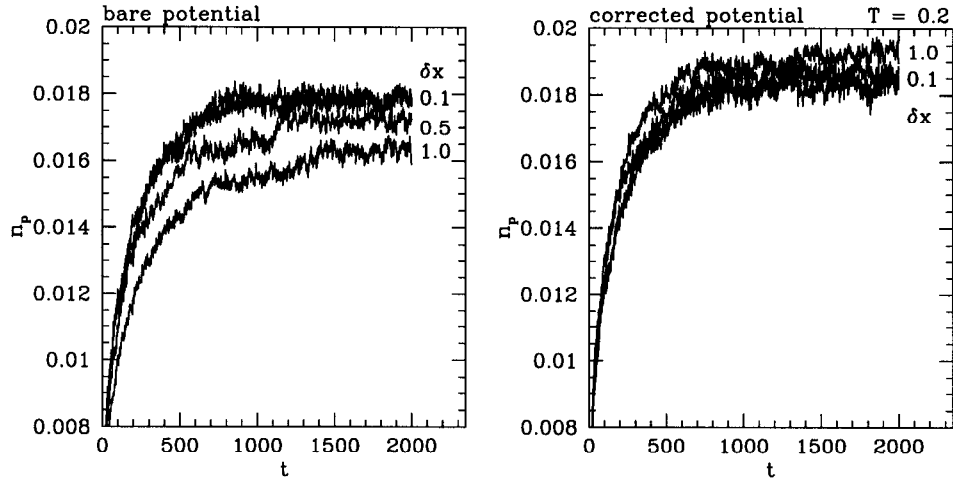


Figure 4: Density of kink-antikinks (half of density of zeros), for  $T = 0.2$  and  $\delta x = 1, 0.5, 0.2$ , and  $0.1$ . The filter cutoff is  $\Delta L = 3$ .